# Supplementary Information

# Structural basis of TRPV4 N-terminus interaction with Syndapin/PACSIN1-3 and $PIP_2$

Benedikt Goretzki[1,2,*], Nina A. Glogowski[1,2,*], Erika Diehl[1,2], Elke Duchardt-Ferner[2,4], Carolin Hacker[2,4], Rachelle Gaudet[3] and Ute A. Hellmich[1,2,§]

*BG and NAG contributed equally

[1]Institute for Pharmacy and Biochemistry, Johannes Gutenberg-Universität Mainz, 55128 Mainz, Germany

[2]Center for Biomolecular Magnetic Resonance (BMRZ), Johann-Wolfgang-Goethe-Universität, 60438 Frankfurt am Main, Germany

[3]Department of Molecular and Cellular Biology, Harvard University, Cambridge, MA 02138, USA

[4]Institute for Molecular Biosciences, Johann-Wolfgang-Goethe-Universität, 60438 Frankfurt am Main, Germany

[§]to whom correspondence should be addressed:
u.hellmich@uni-mainz.de

**Table S1 related to Fig. 2 and Fig. 4: Summary of $K_D$ values for TRPV4 with its interaction partners.** All affinities have been determined through NMR-based chemical shift perturbation assays. Reporter and respective ligand are indicated in the table.

| Reporter | Ligand | Temp. (K) | Method | $K_D$ (µM) |
|---|---|---|---|---|
| $^{15}$N-PACSIN1 SH3 | PRR | 298 | $^{1}$H, $^{15}$N-HSQC | 51.6±7.6 |
| $^{15}$N-PACSIN2 SH3 | PRR | 298 | $^{1}$H, $^{15}$N-HSQC | 12.7±2.4 |
| $^{15}$N-PACSIN3 SH3 | PRR | 298 | $^{1}$H, $^{15}$N-HSQC | 68.6±5.7 |
| $^{15}$N-PACSIN3 SH3 | PBD-PRR | 293 | $^{1}$H, $^{15}$N-HSQC | 54.3±5.2 |
| $^{15}$N-PACSIN3 SH3 | PBD-PRR | 298 | $^{1}$H, $^{15}$N-HSQC | 74.2±11.8 |
| $^{15}$N-PBD-PRR | PACSIN3 SH3 | 298 | $^{1}$H, $^{15}$N-HSQC | 19.3±5.7 |
| $^{15}$N-PBD$^{AAWAA}$-PRR | PACSIN3 SH3 | 298 | $^{1}$H, $^{15}$N-HSQC | 63.8±6.4 |
| $^{15}$N-PACSIN3 SH3 | PBD-PRR (in presence of $PIP_2$) | 293 | $^{1}$H, $^{15}$N-HSQC | 82.6±13.8 |
| $^{15}$N-PACSIN3 SH3 | PBD-PRR_P128A | 298 | $^{1}$H, $^{15}$N-HSQC | 156.2±15.6 |
| $^{15}$N-PACSIN3 SH3 | PBD-PRR_P128A/P129L | 298 | $^{1}$H, $^{15}$N-HSQC | 165.6±12.6 |
| $^{15}$N-PACSIN3 SH3 | PBD$^{AAWAA}$-PRR | 293 | $^{1}$H, $^{15}$N-HSQC | 83.3±5.2 |
| $^{15}$N-PACSIN3 SH3 | PBD$^{AAWAA}$-PRR (in presence of $PIP_2$) | 293 | $^{1}$H, $^{15}$N-HSQC | 79.0±7.9 |
| PI(4,5)$P_2$ dIC8 | PRR | 298 | $^{31}$P 1D | 2230.3±745.5 |
| PI(4,5)$P_2$ dIC8 | PBD-PRR | 298 | $^{31}$P 1D | 139.8±18.9 |
| PI(4,5)$P_2$ dIC8 | PBD$^{AAWAA}$-PRR | 298 | $^{31}$P 1D | 2711.4±108.9 |

**Table S2 related to STAR Methods: TRPV4 N-terminal peptides used in this study.** Site-specifically isotope labeled TRPV4-PRR peptides were commercially obtained from jpt peptide technologies (Berlin, Germany), for purification of others see Materials and Methods.

| Name | Amino Acid Sequence (and residue number) |
|---|---|
| PBD-PRR | $^{105}$ENKRWRRRVVEKPVAGTKGPAPNPPPVLKV$^{134}$ |
| PBD$^{AAWAA}$-PRR | $^{105}$ENAAWAARVVEKPVAGTKGPAPNPPPVLKV$^{134}$ |
| PBD-PRR_P128A | $^{105}$ENKRWRRRVVEKPVAGTKGPAPNAPPVLKV$^{134}$ |
| PBD-PRR_P128A/P129L | $^{105}$ENKRWRRRVVEKPVAGTKGPAPNALPVLKV$^{134}$ |
| PRR | $^{121}$TKGPAPNPPPVLKV$^{134}$(W$^{\#}$) |
| PRR_V131I | $^{121}$TKGPAPNPPPILKV$^{134}$(W$^{\#}$) |
| $^{13}$C,$^{15}$N-Pro124 Ala125 PRR | $^{121}$TKGP*A*PNPPPILKV$^{134}$(W$^{\#}$) |
| $^{13}$C-Pro126 PRR | $^{121}$TKGPAP*NPPPILKV$^{134}$(W$^{\#}$) |
| $^{13}$C-Pro128 PRR | $^{121}$TKGPAPNP*PPILKV$^{134}$(W$^{\#}$) |
| $^{13}$C-Lys122 Pro130 PRR | $^{121}$TK*GPAPNPPP*ILKV$^{134}$(W$^{\#}$) |
| $^{13}$C-Pro129 Lys133 PRR | $^{121}$TKGPAPNPP*PILK*V$^{134}$(W$^{\#}$) |

* selectively labeled residue

# the C-terminal Trp residue was added to the peptides for concentration determination purposes.

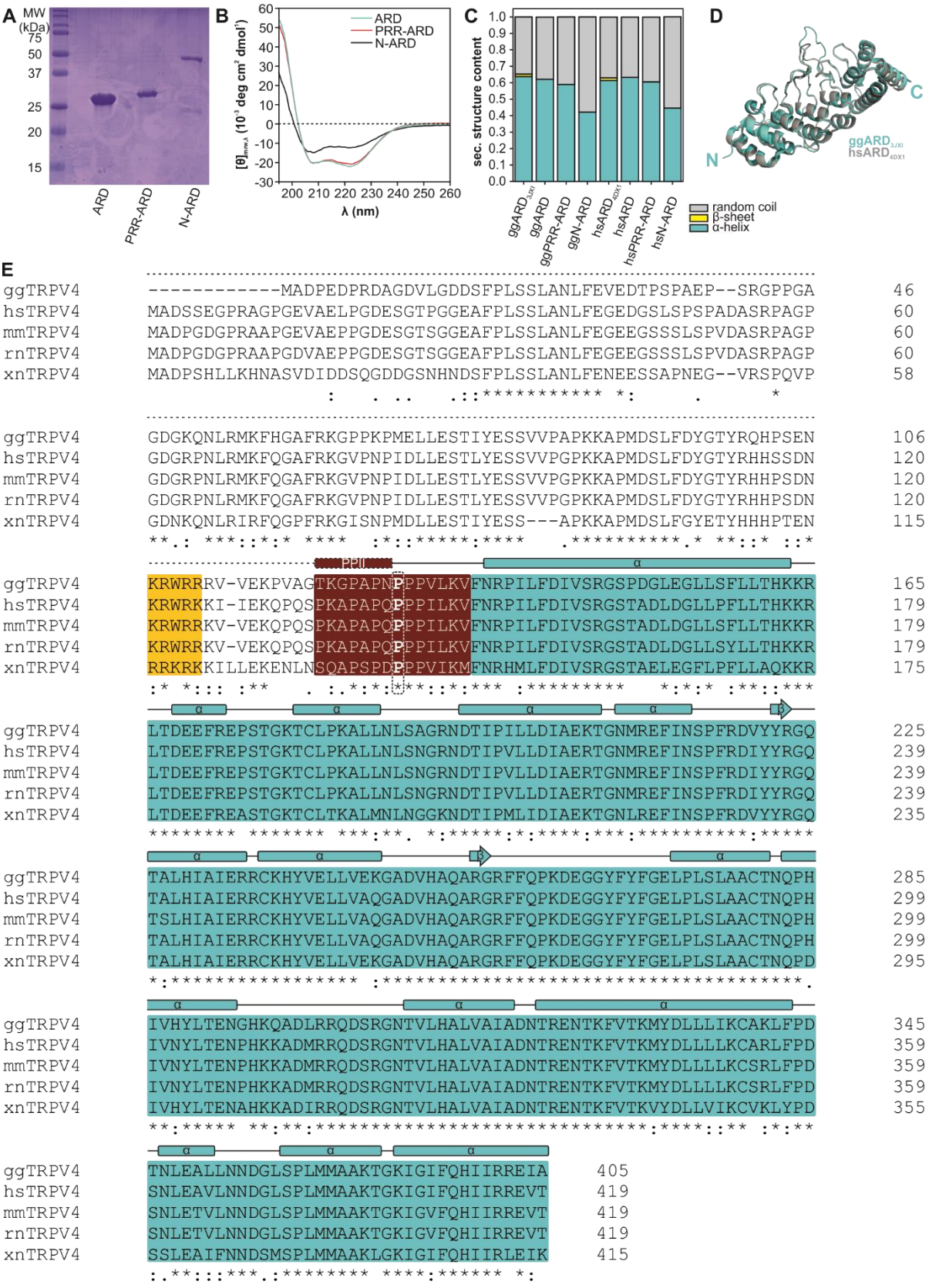


**Figure S1 related to Fig. 1: Structural analysis of the human TRPV4 N-terminus.** (A) Coomassie-stained SDS-PAGE of purified human TRPV4 N-terminal constructs and (B) CD spectra of purified proteins comprising the entire N-terminus (N-ARD; residues 1-383), the Ankyrin repeat domain with the PRR (PRR-ARD; residues 122-383), and the isolated ankyrin repeat domain (ARD; residues 134-383). Importantly, and as observed for the chicken TRPV4 N-terminus (Fig. 1), the proximal N-terminus is unstructured in human TRPV4. (C) CD spectroscopy based secondary structure prediction of purified TRPV4 N-terminal constructs ARD, PRR-ARD and N-ARD from chicken and human using the BeStSel method (Micsonai et al., 2015).

Addition of the proximal 132 residues to the ARD increases the contribution of random coil and reduces the α-helical content in the spectrum by about one third. The predicted α-helix/β-sheet/random coil content of the purified constructs is 62.1/0/37.8% for ggARD, 59.0/0/41.0% for ggPRR-ARD, 42.2/0/57.8% for ggN-ARD, 63.3/0/36.6% for hsARD, 60.5/0/39.4% for hsPRR-ARD and 44.6/0/55.5% for hsN-ARD. For comparison, the secondary structure content of the chicken and human ARD was determined from the crystal structures shown in D (64/1.6/34.7% for chicken ARD, PDB: 3JXI, and 61.4/1.6/36.9% for human ARD, PDB: 3DX1). (D) Overlay of human (grey, PDB: 4DX1) and chicken TRPV4-ARD (cyan, PDB: 3JXI) crystal structures highlighting the α-helical character of this domain. (E) Sequence alignment (Clustal Omega) of chicken (*Gallus gallus*, gg, UniProtKB: A0A1D5PXA5), human (*Homo sapiens*, hs, UniProtKB: Q9HBA0), rat (*Rattus norwegicus*, rn, UniProtKB: Q9ERZ8), mouse (*Mus musculus*, mm, UniProtKB: Q9EPK8) and frog (*Xenopus tropicalis*, xn, UniProtKB: 7BWY7) TRPV4 N-terminus. The ++W++ motif important for $PIP_2$ binding (Garcia-Elias et al., 2013) and the proline rich region relevant for the interaction with PACSINs (Cuajungco et al., 2006; D'hoedt et al., 2008) are highlighted in yellow and russet respectively. Pro128 (*Gallus gallus* sequence nomenclature), which adopts a *cis* conformation when bound to PACSIN SH3 (Fig. 3), is conserved across species (dashed frame). The polyproline helix type II (PPII) is indicated in red, the Ankyrin repeat domain (ARD) is shown in cyan.

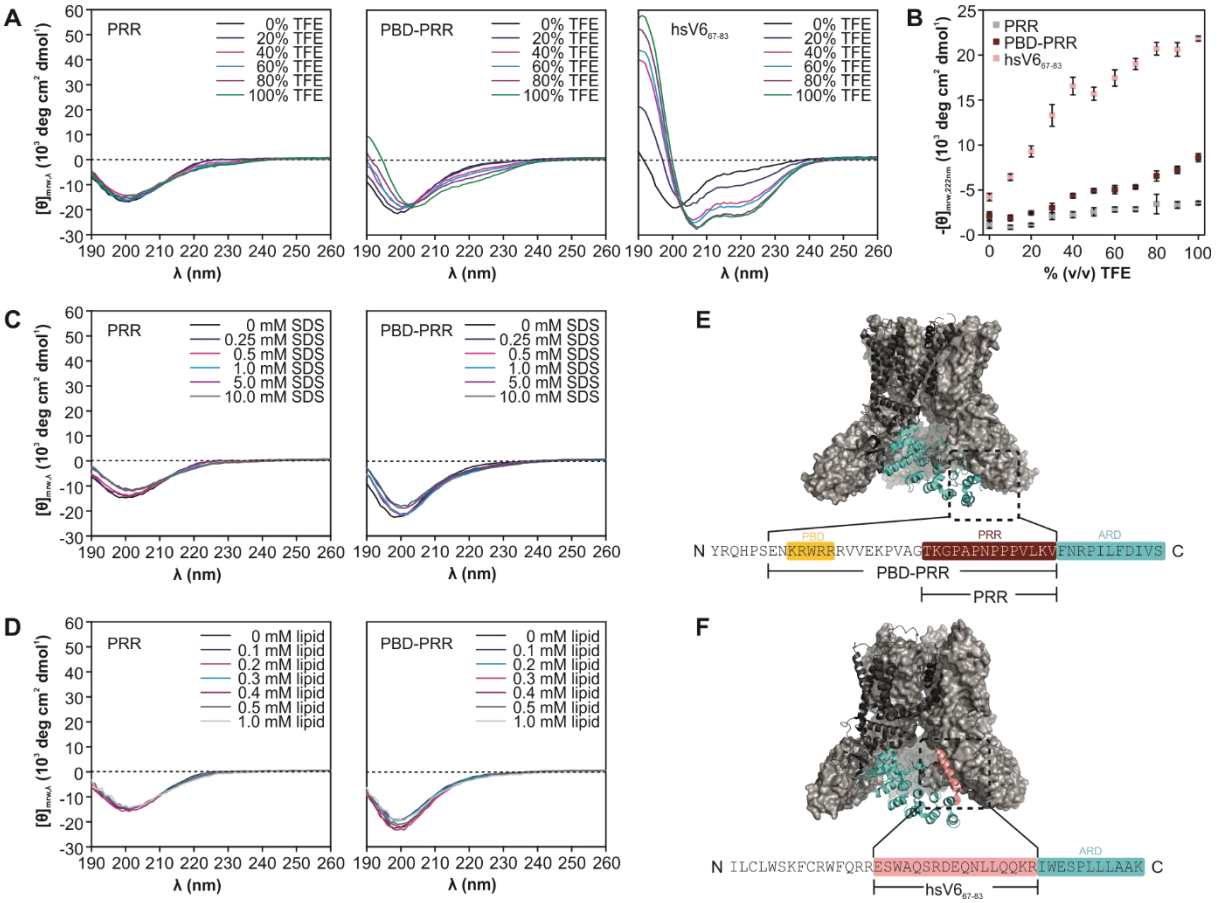


**Figure S2 related to Fig. 1: CD spectroscopic analysis of the TRPV4 N-terminus.** (A) CD spectra of *Gallus gallus* TRPV4 proline rich region (PRR), $PIP_2$ binding domain in combination with PRR (PBD-PRR) and the respective region from the *Homo sapiens* TRPV6 ion channel (hsV6$_{67-83}$). Increasing amounts of trifluoroethanol (TFE) were added to promote hydrogen bond formation. Of note, TRPV4-PRR does not show any changes in the spectrum which would agree with a polyproline helix. Spectral changes are observable in the longer construct containing the PBD in addition to the PRR and the TRPV6 peptide. (B) The mean residue ellipticity at 222 nm (signifying α-helical content) is shown with increasing TFE concentrations for the three peptides. While the TRPV6 peptide easily adopts an α-helical fold, TRPV4-PRR and PBD-PRR do not, even at the highest TFE concentrations (errors represent standard deviations based on three independent measurements). (C) CD spectroscopy of TRPV4 N-terminal peptides with increasing amounts of SDS and (D) net negatively charged liposomes (POPC:POPG, 1:3 mol/mol). Increasing amounts of membrane mimetics or lipid membranes does not lead to secondary structure formation. (E) Structure of *Xenopus tropicalis* TRPV4 (PDB: 6BBJ) highlighting location and sequence of TRPV4 N-terminus used for CD spectroscopy. Of note, the sequence shown in the inset is the *Gallus gallus* sequence used in our experiments. The N-terminal region investigated here is not resolved in the available structures from TRPV1, TRPV2 and TRPV4 (Liao et al., 2013; Zubcevic et al., 2016; Deng et al., 2018) and is α-helical in the structures of TRPV5 and TRPV6 (Hughes et al., 2018; McGoldrick et al., 2018). (F) Structure of TRPV6 (PDB: 5WO7) highlighting the N-terminal region used for CD spectroscopy.

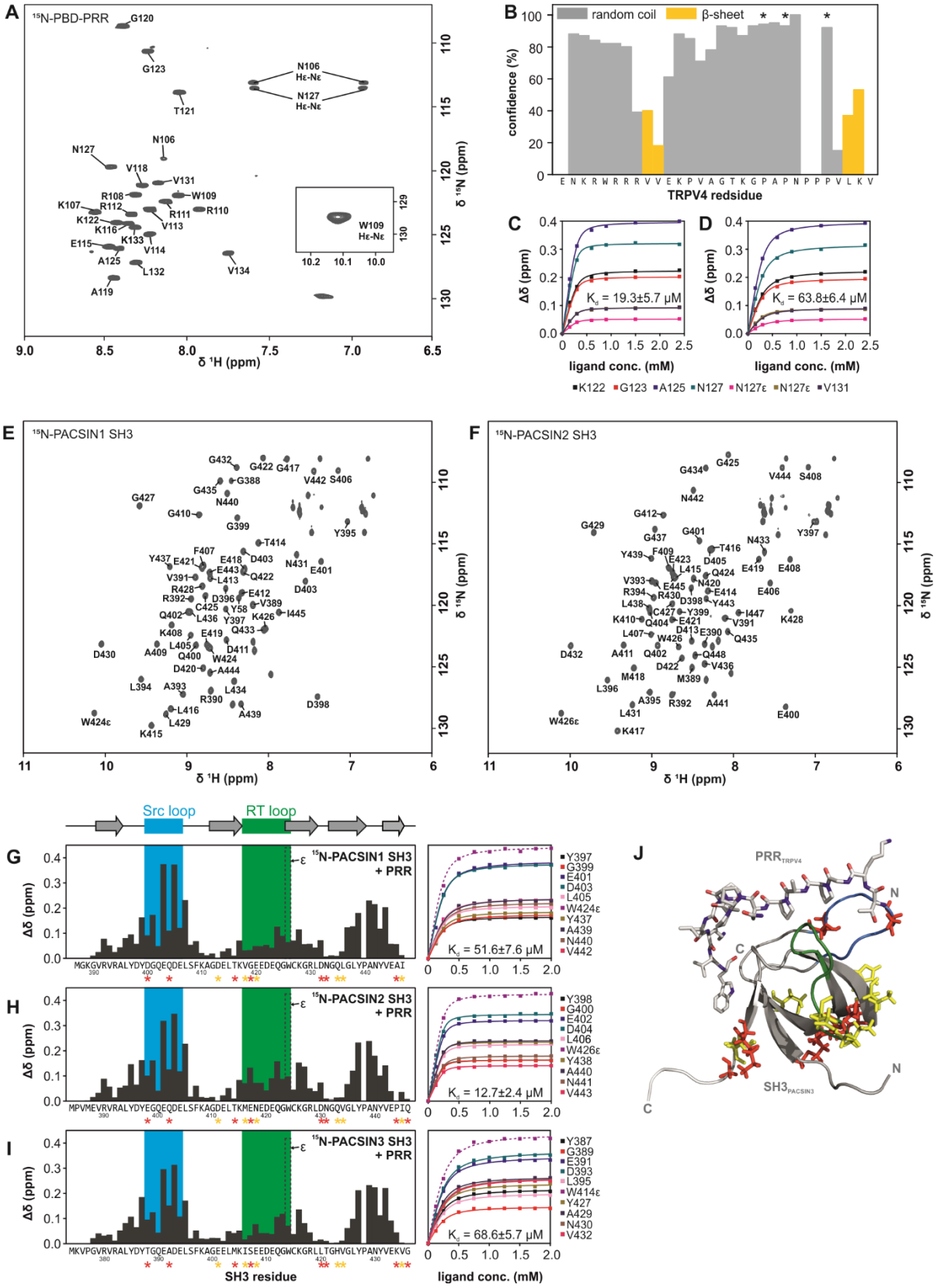


**Figure S3 related to Fig. 2: NMR-based structural analysis of PACSIN-SH3 interaction with TRPV4-PRR** (A) $^{1}$H, $^{15}$N-HSQC of *Gallus gallus* TRPV4 N-terminal region comprising the proline rich region and $PIP_2$ binding domain ($^{15}$N-PBD-PRR). Residue numbering is based on the residue count in the full-length TRPV4 channel. (B) Secondary structure prediction of TRPV4-PBD-PRR based on chemical shifts (HN, Cα, Cβ, Co) using TALOS+ (Shen et al., 2009). The NMR structure prediction (in agreement with CD spectroscopic data, Fig. S2) shows that the TRPV4-PBD-PRR is an overall unstructured region of the protein. For several proline residues in the PRR (*), the predicted torsion angles agree with a PPII helical structure (PPII torsion angles: ϕ ≈ -75°, ψ ≈ 145°; P124: ϕ = -72.0°, ψ = 147.5°; P126: ϕ = 73.6°, ψ = 147.5°; P130: ϕ = -78.7°, ψ = 146.3°). (C) Titration of $^{15}$N-

PBD-PRR with unlabeled PACSIN3 SH3 domain leads to chemical shift changes which are plotted to determine the affinity between both partners (19.3 ± 5.7 μM). (D) Affinity between $^{15}$N-PBD$^{AAWAA}$-PRR and PACSIN3 SH3 domain was calculated to be 63.8 ± 6.4 μM. (E) $^{1}$H, $^{15}$N-HSQC and backbone assignments of (A) *Gallus gallus* PACSIN1 SH3 domain and (F) *Gallus gallus* PACSIN2 SH3 domain. Residue numbering is based on the residue count in the full-length PASCINs (for sequences, secondary structure prediction and chemical shift perturbation experiments, see also Fig. S5 and S6). Chemical shift perturbations of (G) $^{15}$N-PACSIN1 SH3, (H) $^{15}$N-PACSIN2 SH3 and (I) $^{15}$N-PACSIN3 SH3 with TRPV4-PRR. To guide the eye, the SH3 domain secondary structure is highlighted at the top, marking the Src loop and RT loop in blue and green respectively. Of note, the side-chain NHε chemical shift perturbation of the tryptophan residue in the RT loop of all three PACSIN SH3 domains is indicated by a dashed bar. Affinities between TRPV4-PRR with all three PACSIN SH3 domains could be determined by mapping chemical shift perturbations of select residues and are found to be in a similar range (51.6 ± 7.6 μM, 12.7 ± 2.4 μM and 68.6 ± 5.7 μM, respectively). (J) Structure of PACSIN3 SH3 domain with TRPV4-PRR highlighting sequence differences between the three PACSIN SH3 domains (see asterisks below sequences in A-C, with yellow asterisks marking less conservative changes and red asterisks more conservative changes). Of note, all differences are found on the back of the SH3 domain, except for two residues in the Src loop, both of which seem to be only marginally affected by TRPV-PRR binding based on chemical shift perturbation data (compare $\Delta\delta$ [ppm] values in G-I).

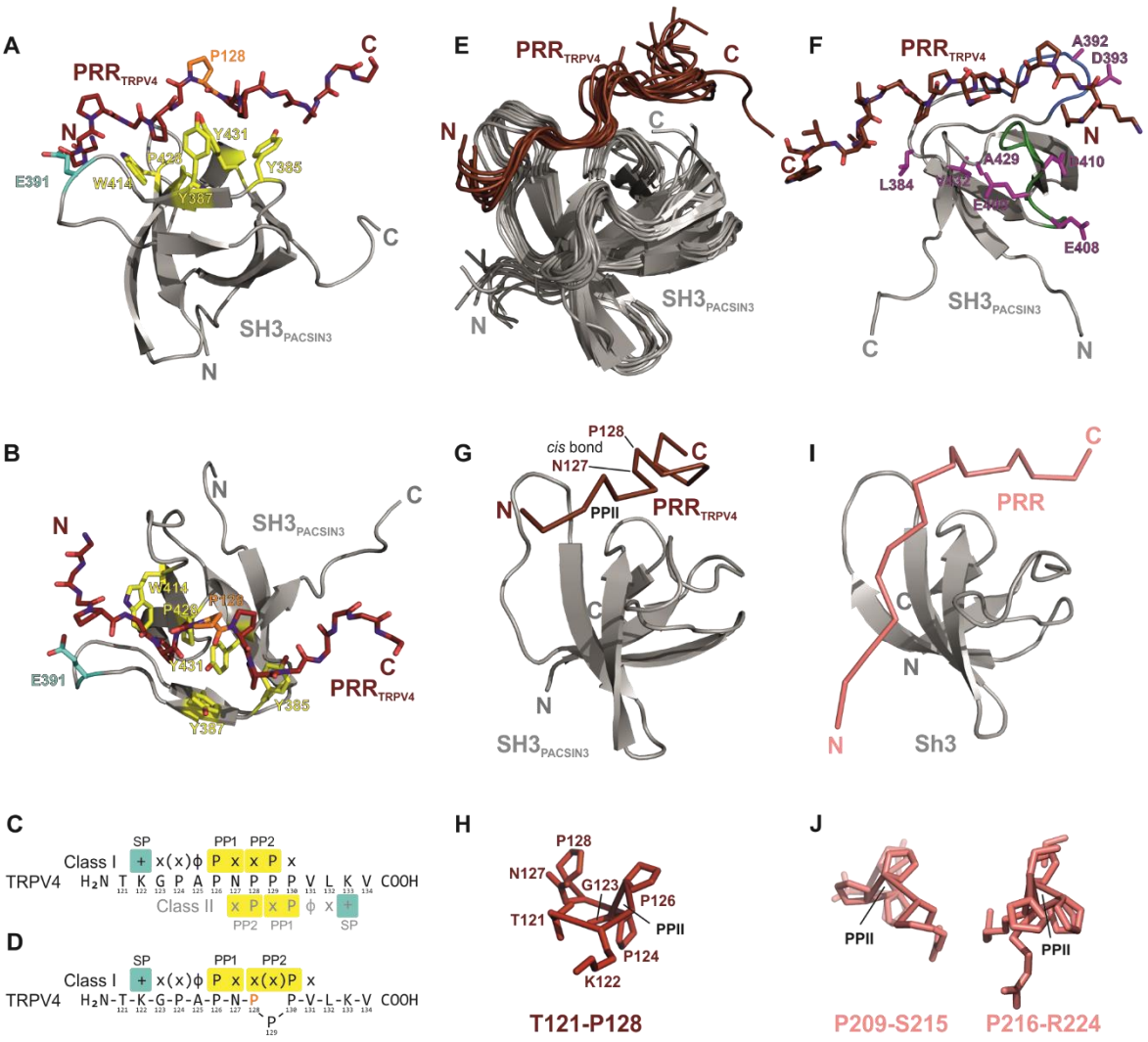


**Figure S4 related to Fig. 3: Structural details of TRPV4-PRR interaction with PACSIN3-SH3 domain**. (A) Top view and (B) side view of PACSIN3 SH3 domain (grey) interacting with TRPV4-PRR (orange). Residues contributing to the SH3 domain's specificity pocket (cyan, E391) and proline pockets (yellow, Y385, Y387, W414, P428, Y431) are highlighted. (C) SH3 domains can interact with substrates in a class I or class II binding mode, with proline residues and a positively charged amino acid of the substrate interacting with the proline pocket 1 and 2 (PP1, PP2) and the specificity pocket (SP) of the SH3 domain. The respective binding mode changes the orientation of the target protein by 180°. The PxxP motif in the TRPV4-PRR is flanked by lysine residues at both sides thereby making it impossible to assign the TRPV4-PRR as a class I or II SH3 substrate based on amino acid sequence. (D) Our structure shows that the TRPV4-PRR binds in a class I motif, and Pro126 dips into the first proline pocket, but due to the *cis* conformation of Pro128, Pro130 rather than Pro129 interacts with the second proline pocket. (E) NMR structure bundle comprising the best 10 structures. (F) Several residues (violet) in the PACSIN3 SH3 domain show variations in chemical shift perturbation upon binding of either PRR or PBD-PRR (compare Fig. S6). Residues E408, E409 and D410 in the RT loop form the so called under-groove (Luo et al., 2016). (G, H) Cartoon representation highlighting the break of the polyproline helix at residue Pro128 compared to (I, J) an SH3 domain interacting with a class I polyproline helix throughout (PDB shown is 2P4R).

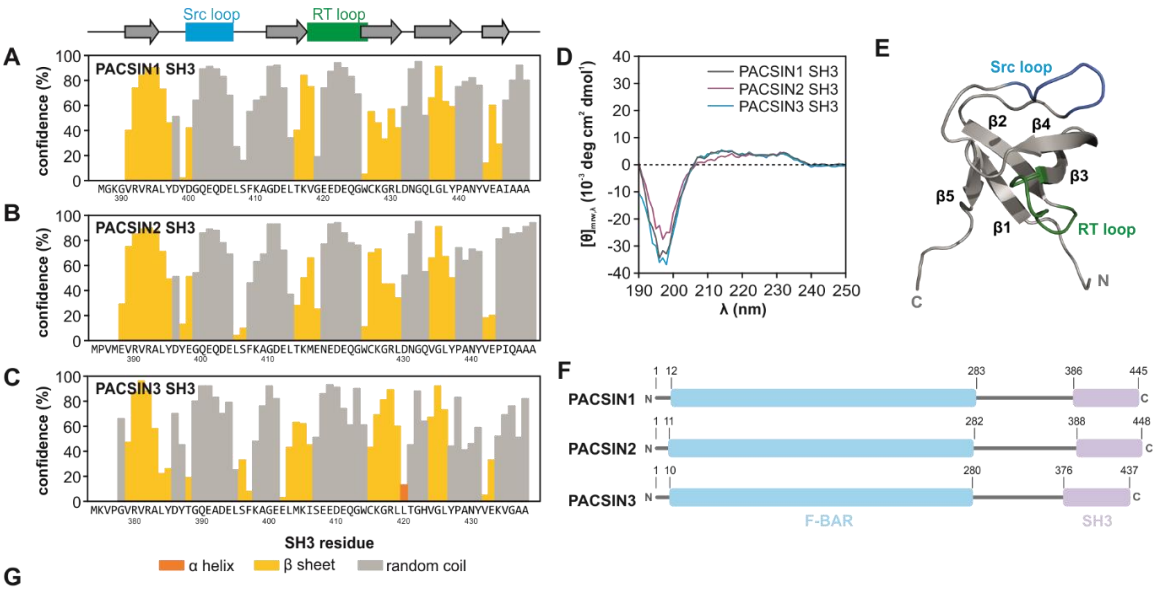


G

```
PACSIN1      MSGSYDESAAAAEETTDSFWEVGNYKRTVKRIDDGHRLCNDLMNCVHERAKIEKSYAQQL   60
PACSIN2      MSGSYDDSVG-VEVSSDSFWEVGNYKRTVKRIDDGHRLCNDLMNCIHERARIEKVYAQQL   59
PACSIN3      MSS---EDDAGGEAPEGSFWEAGNYRRTVKRVDDGYRLCNDLISCFQERAKIEKNYAQQL   57
             **.   :. .  *   .****.***:*****:***:******:.*.:***:*** *****

PACSIN1      TDWSKRWRQLIEKGPQYGSLERAWGAIMTEADKVSELHQEVKNSLLNDDFEKVKNWQKDA   120
PACSIN2      TEWAKRWKQLVEKGPQYGTVERAWCAFMSEAEKVSELHLEVKGSLMNEDFEKIKNWQKEA   119
PACSIN3      TEWSRKWRTNVEKGPQYGTLEKAWHAFLTAADKLSEIHLVVRNHLAGEDSDKIKAWQKEA   117
             *:*:::*:  :********::*:** *::: *:*:***:*  *:. * .:* :*:* ***:*

PACSIN1      YHKQIMGGFKEAKEAEDGFRKAQKPWAKKLKELETAKKAYHLACKEEKLAMTREANSKAD   180
PACSIN2      FHKQMMGGFKETKEAEDGFRKAQKPWAKKLKEVEAAKKAYHAACKEEKLAISRETNSKAD   179
PACSIN3      YHKQIIGGFKETKEAEDGFRKAQKPWVKKMKDVETSKKNYHAARKEEKTAHTRENHAKAD   177
             :***::*****:**********:***.**:*:*:*::** ** * **** * :** ::***

PACSIN1      QSNTPEQQKKLQDKVEKCKQDVQKTQEKYEKVLDELNKCTPQYMESMEQVFEQCQQFEEK   240
PACSIN2      PALNPEQLKKLQDKVERSKQDVLKTKAKYEKSLKELDNATPQYMENMEQVFEQCQQFEEK   239
PACSIN3      SSVSQEQLRKLQERVEKCTQEAEKCKDQYEKMLEELNRYNPRYMEDMEQVFEGCQEAERK   237
              : . ** :***::**:..*:. * :  :*** *.**:. .*:***.****** **: *.*

PACSIN1      RLNFLKEVLLDIKRHLNLAESSSYANVYRELEQTIRLSDAQEDLRWFRSTSGPGMPMNWP   300
PACSIN2      RLRFFREVLLEVQKHLDLSNVASYKNIYRELEQNIKTADAVEDLRWFRANQGPGMSMNWP   299
PACSIN3      RLCFFKEMFLNLHQHLNLSTSESFQALYRDLYQVIMAADNQEDLKWWRNTHGPGMAMNWP   297
             ** *::*::*::::**:*:   *:  :**:* * *  :*  ***:*:* . **** ****

PACSIN1      QFE--EWNPDLTHTITRKEKMK-KGEGVTLTNASSTGESGASAGERGSVSSHDRGQTYSA   357
PACSIN2      QFEDDEWSADLNRTLSRREKKK-ASDGVTLTGINQTGDQVSQPNKHSSVSSYEKNQSYPT   358
PACSIN3      QFE--EWSLETQRPITKKEKSGKVADDVTLTSILPTRDGVVSQTPL--QTRQGGGKEDIS   353
             ***  **. :  : :::::**    .:.****.   * :   .       :    .:   :

PACSIN1      EWSDDEGSNSFNASEANGGTNPFDEDSA-GKGVRVRALYDYDGQEQDELSFKAGDELTKL   416
PACSIN2      DWSDEESNNPFSSTDAKGDTNPFDEDTSPVMEVRVRALYDYEGQEQDELSFKAGDELTKM   418
PACSIN3      EWSDEDTPKKYLD--ANGH-----EEDIKVPGVRVRALYDYTGQEADELSFKAGEELMKI   406
             :***::  : :    *:*      *:      ********* *** ********:** *:

PACSIN1      GEEDEQGWCKGRLDNGQLGLYPANYVEAI--   445
PACSIN2      ENEDEQGWCKGRLDNGQVGLYPANYVEPIQ-   448
PACSIN3      SEEDEQGWCKGRLLTGHVGLYPANYVEKVGL   437
              :****** ***** .*::******** :
```

**Figure S5 related to Fig. 3: Structure analysis of the PACSIN1-3 SH3 domains.** Secondary structures of Gallus gallus (A) PACSIN1 SH3 (B) PACSIN2 SH3 and (C) PACSIN3 SH3 domains calculated with TALOS+ (Shen et al., 2009) based on NMR assignments (Fig. 2, Fig. S3). All three PACSIN SH3 domains show the expected SH3 domain topology. (D) CD spectra of all three PACSIN SH3 domains highlighting the high α-sheet content of these proteins. (E) Solution NMR structure of PACSIN3 SH3 domain, highlighting the respective orientations of the Src and RT loops and the five β-strands. (F) Topology model for PACSIN1-3. (G) Sequence alignment (Clustal Omega) of Gallus gallus PACSIN1 (UniProtKB: E1C4P4), PACSIN2 (UniProtKB: O13154) and PACSIN3 (UniProtKB: Q1G1I6). Each PACSIN consists of an F-BAR domain (blue) connected to a C-terminal SH3 domain (grey). Regions proposed to be involved in F-BAR/SH3 domain interactions (Rao et al., 2010) are boxed. Importantly, for the SH3 domain, these are exactly the residues interacting with the TRPV4-PRR (see also Fig. 4A, Fig. S4 and Fig. S6).

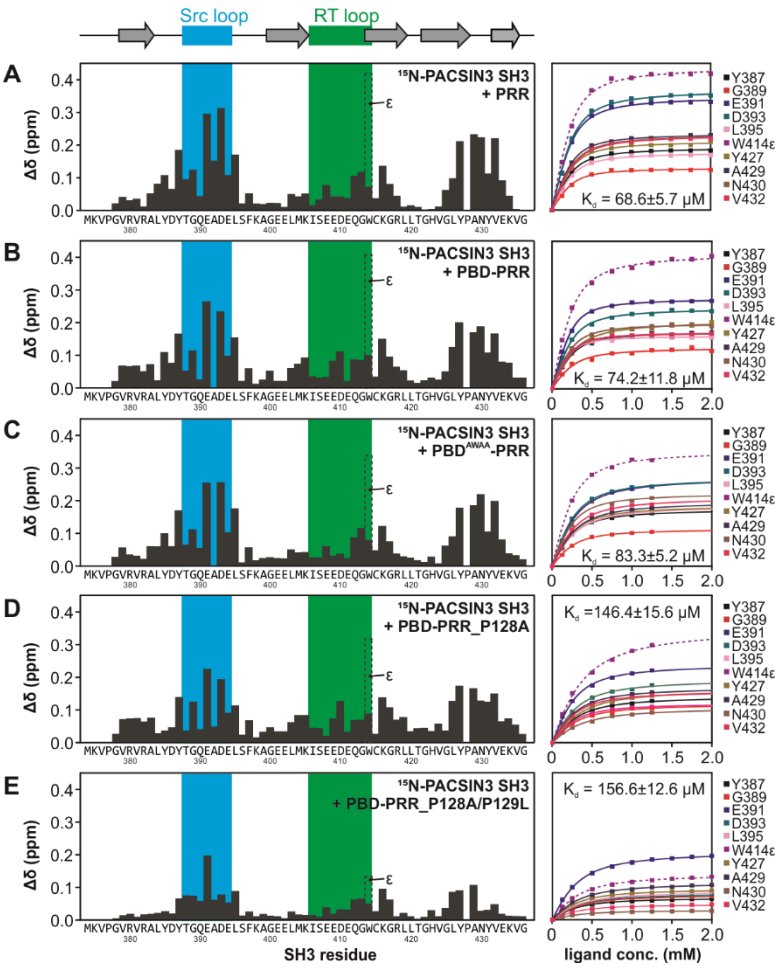


**Figure S6 related to Fig. 3: Comparison of chemical shift differences between different TRPV4 N-terminal peptides binding to PACSIN3 SH3 domain.** (A) Interaction of $^{15}$N-labeled PACSIN3 SH3 domain with (A) TRPV4-PRR overall leads to the same chemical shift differences as (B) titration of the isotope labeled SH3 domain with a peptide containing both the PRR and the $PIP_2$ binding domain (PBD-PRR). Of note, small differences can be observed in the Src loop and in a basic patch in the RT loop (residues E408 and following) (see also Fig. S4F). Likewise, (C) introduction of a mutation in the PBD that abrogates lipid interaction ($^{107}$AAWAA$^{111}$) (Garcia-Elias et al., 2013) does not significantly affect PACSIN3 SH3 domain binding. (D, E) Introduction of the P128A single or P128A/P129L double mutant reduces the interaction of the TRPV4-PRR with PACSIN3 SH3 but does not completely abrogate it.